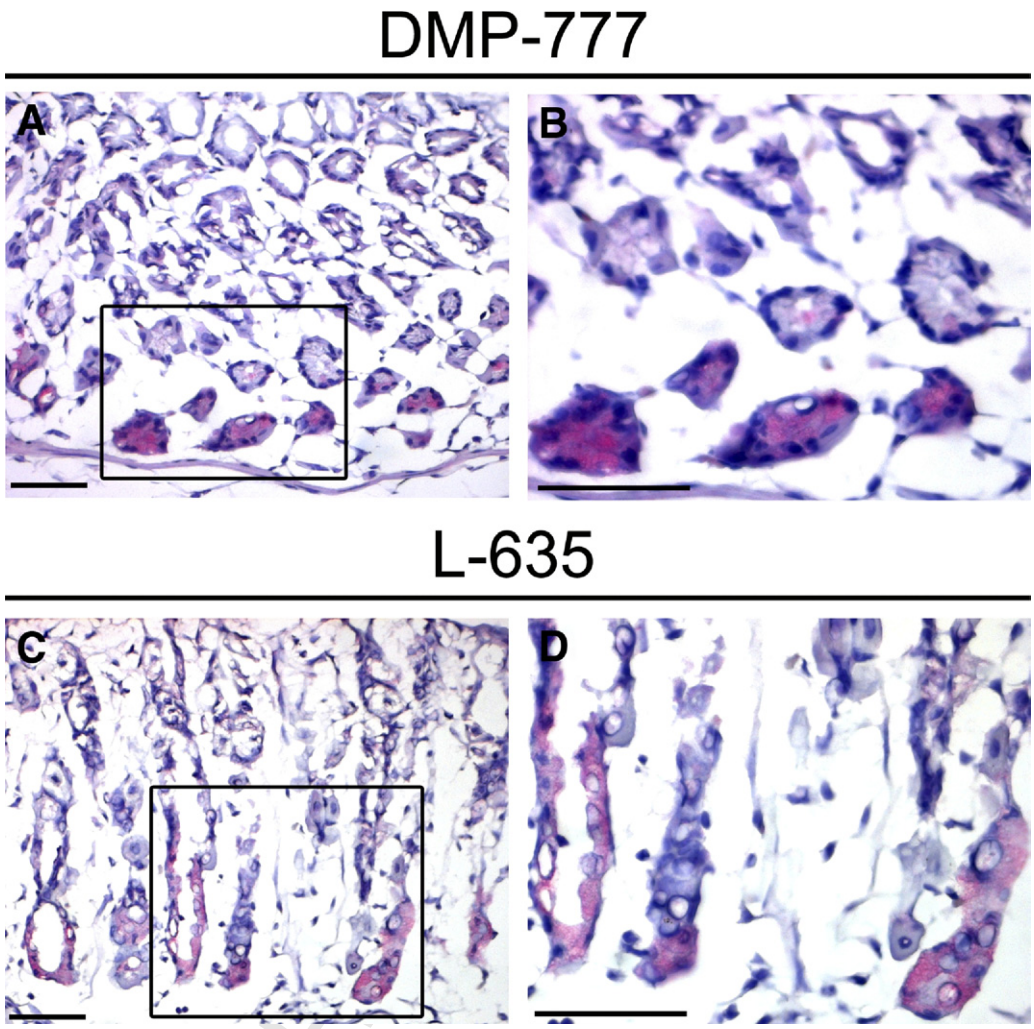

Supplementary Figure 1. Expression of β-galactosidase in Mist1$^{CreER/+}$/Rosa26R^{LacZ} mice treated with DMP-777 and L-635. To identify expression of β-galactosidase protein in Mist-Cre$^{ER/+}$/Rosa26R^{LacZ} mice after treatment with DMP-777 and L-635, we immunostained gastric tissues with antibodies against β-galactosidase (Vector Red staining). (*A*) In DMP-777–treated mice, we observed β-galactosidase expression at the bases of fundic glands. (*B*) Higher magnification view of panel *A*. (*C*) As seen with X-gal staining, β-galactosidase expression was observed in L-635–treated mice along the entire gland length. (*D*) Higher magnification view of panel *C*. Bar, 50 μm.

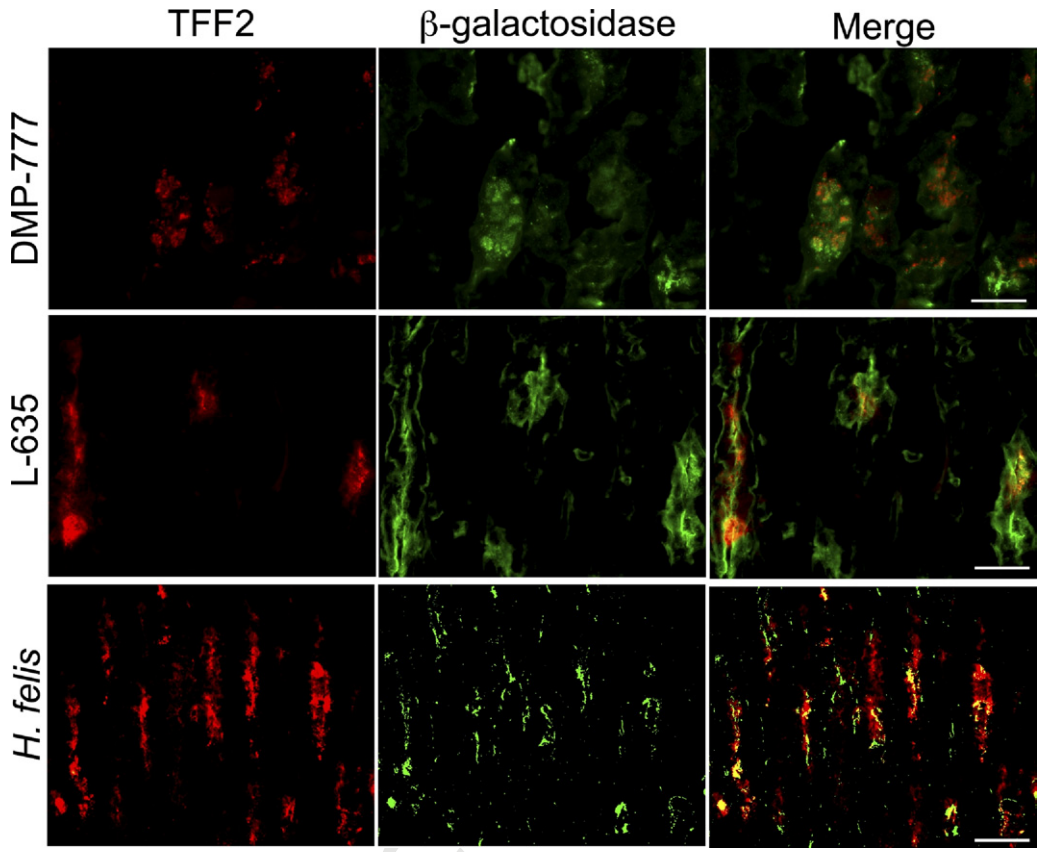

Supplementary Figure 2. Dual immunostaining for TFF2 (red) and bacterial β-galactosidase (green) in mouse models of metaplasia. Mist1$^{CreER/+}$/Rosa26R^{LacZ} mice were treated with 3 doses of tamoxifen to induce β-galactosidase expression in mature chief cells and after a 10-day, drug-free interval, metaplasia was induced with 3 different protocols: 14 days of DMP-777, 3 days of L-635, or 6 months' infection with *H felis*. Frozen sections of gastric fundus were dual immunostained for TFF2 (red) and bacterial β-galactosidase (green). A dual staining overlay is shown at the right. Bar, 50 μm.

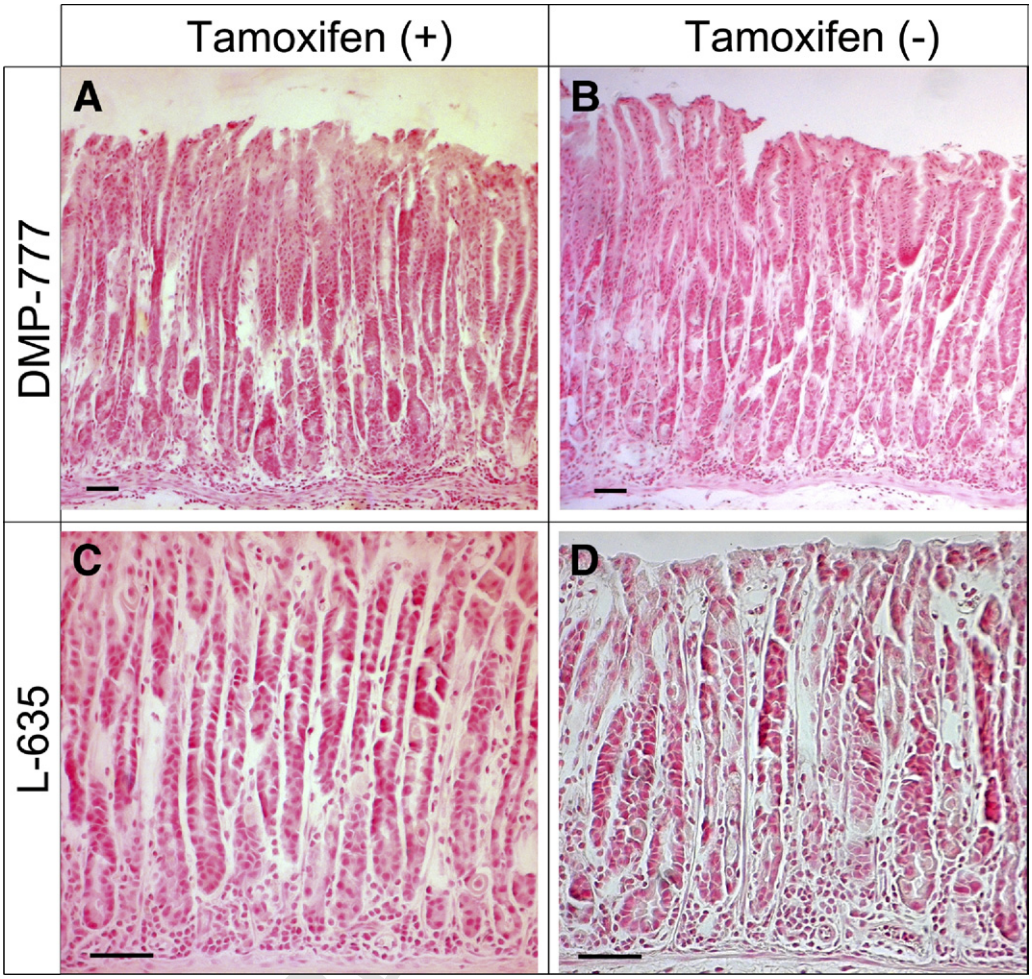

Supplementary Figure 3. No expression of β-galactosidase in Rosa26R^{LacZ} mice treated with DMP-777 and L-635 without or with tamoxifen treatment. To confirm whether endogenous β-galactosidase activity was induced in Rosa26R^{LacZ} mice after treatment with DMP-777 (n = 2) and L-635 (n = 2), we evaluated the β-galactosidase activity by incubation of tissue from mice that either never received tamoxifen (n = 2) or were treated with 3 doses of tamoxifen (n = 2). β-galactosidase activity was visualized by incubation of stomachs with X-gal followed by paraffin-embedding and sectioning. No β-galactosidase expression was observed in the entire stomach including fundic glands after treatment with either (*A* and *B*) DMP-777 or (*C* and *D*) L-635. Bar, 50 μm.

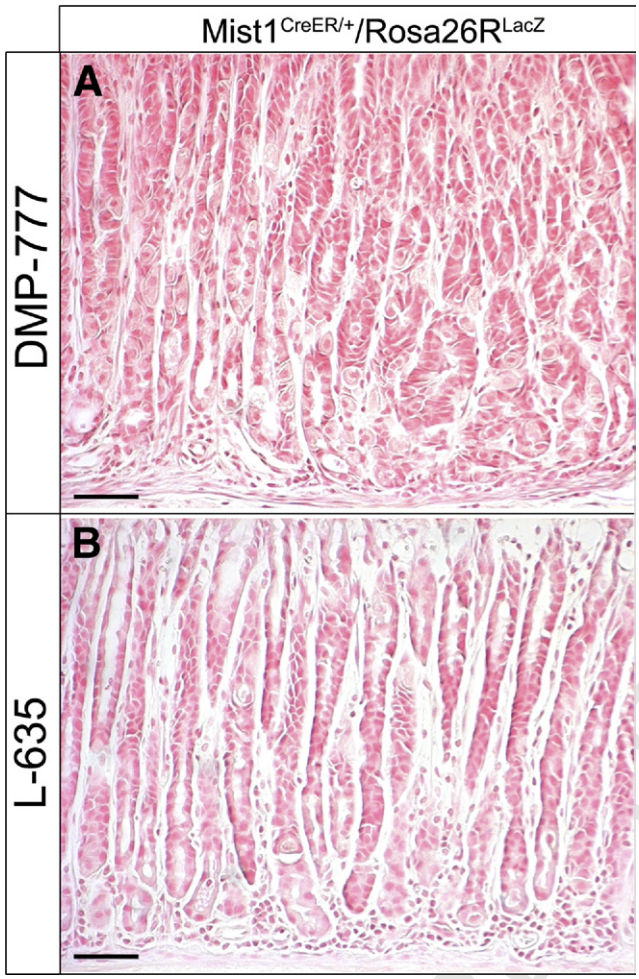

Supplementary Figure 4. No expression of β-galactosidase in Mist1$^{CreER/+}$/Rosa26R^{LacZ} mice treated with DMP-777 and L-635 without tamoxifen treatment. To confirm whether endogenous β-galactosidase activity was induced in Mist1$^{CreER/+}$/Rosa26R^{LacZ} mice after treatment with DMP-777 (n = 2) and L-635 (n = 2), we evaluated the β-galactosidase activity by incubation of tissue from mice that never received tamoxifen. β-galactosidase activity was visualized by incubation of stomachs with X-gal followed by paraffin-embedding and sectioning. No β-galactosidase expression was observed in the entire stomach including fundic glands after treatment with either (*A*) DMP-777 or (*B*) L-635. Bar, 50 μm.

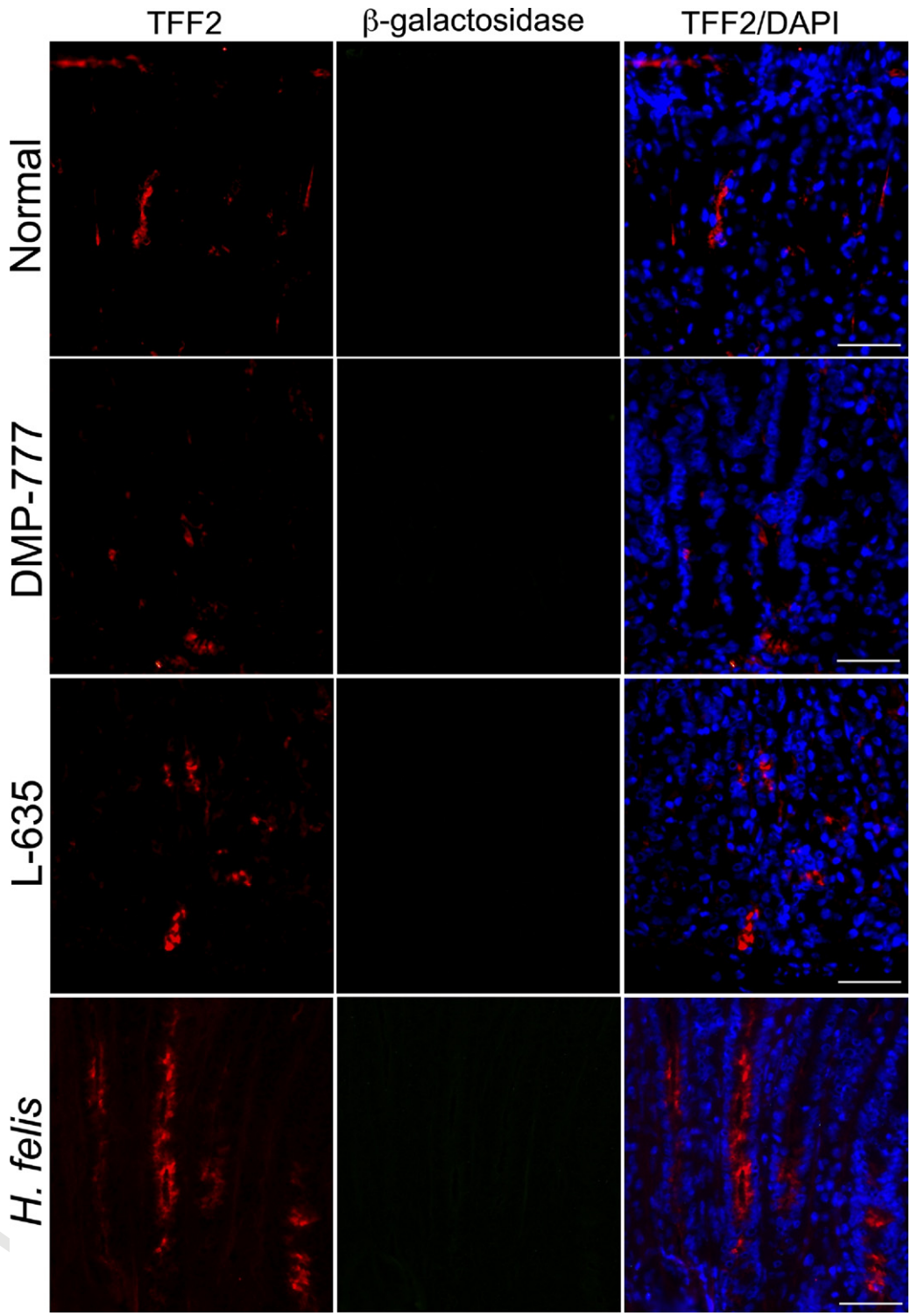

Supplementary Figure 5. Induction of SPEM in mice does not induce spurious β-galactosidase immunostaining. Mice were maintained either without treatment (normal) or were treated with 14 days of DMP-777 (n = 2), 3 days of L-635 (n = 2), or 6 months' infection with *H felis* (n = 2). Frozen sections of gastric fundus were dual immunostained for TFF2 (red) and bacterial β-galactosidase (green). A dual staining overlay of TFF2 and 4,6-diamidino-2-phenylindole (DAPI) is shown at the right. No immunostaining for β-galactosidase was observed in gastric sections with any treatment protocol. Bar, 50 μm.

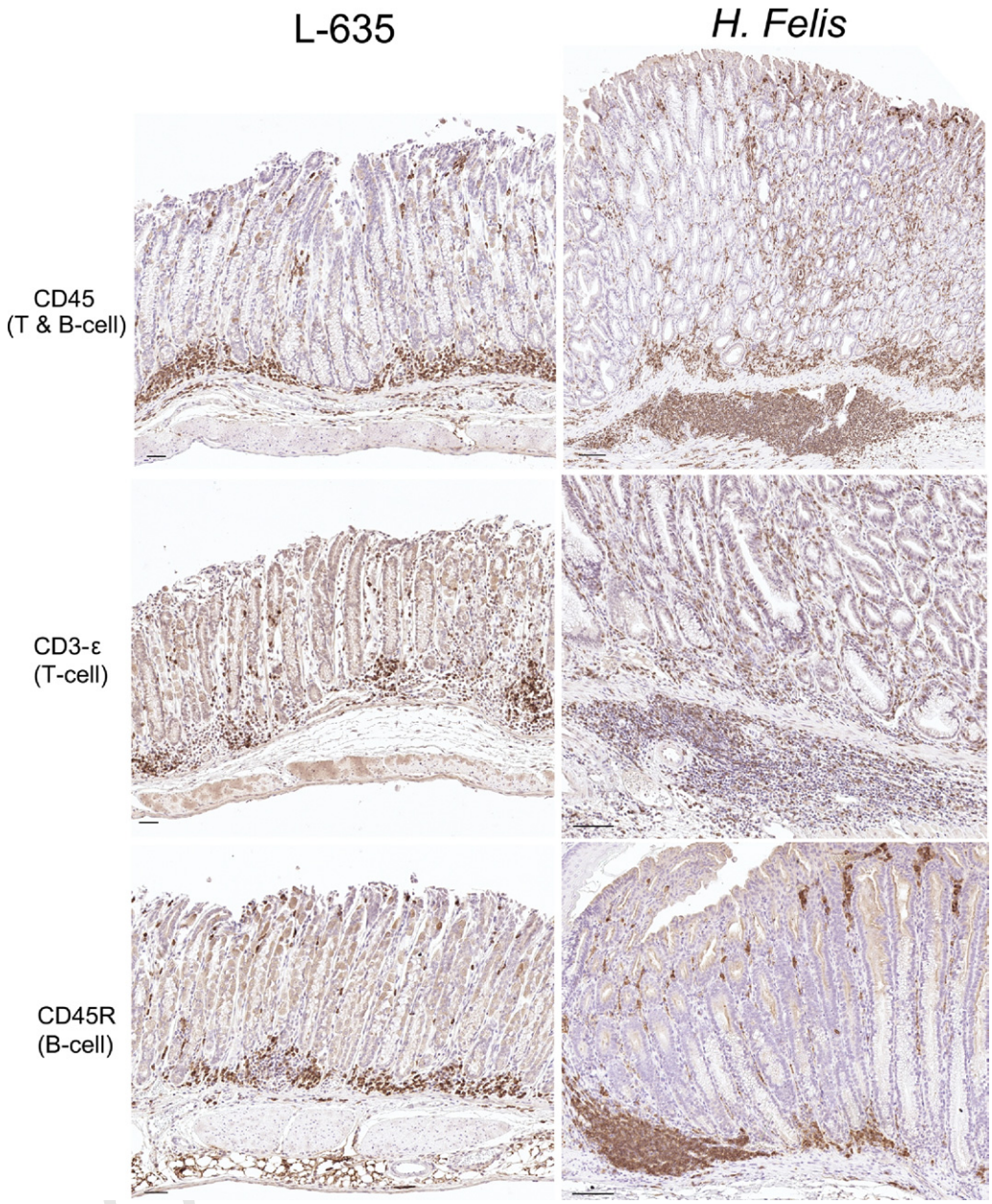

Supplementary Figure 6. Characterization of infiltrating inflammatory cells in SPEM models with inflammation using lymphocyte cell-surface antigen markers restricted to the T- and B-cell lineage. In sections of mouse stomachs from L-635–treated or *H felis*–infected mice, general lymphocyte staining of both B and T cells was determined with CD45 immunostaining (a general immune cell marker), T-cell–specific staining was performed for CD3-ε and B-cell–specific staining was performed with antibodies against CD45R. Both T-cell and B-cell staining was observed in both SPEM models with inflammation in the mucosa as well as in the submucosa. Bar, 50 μm.

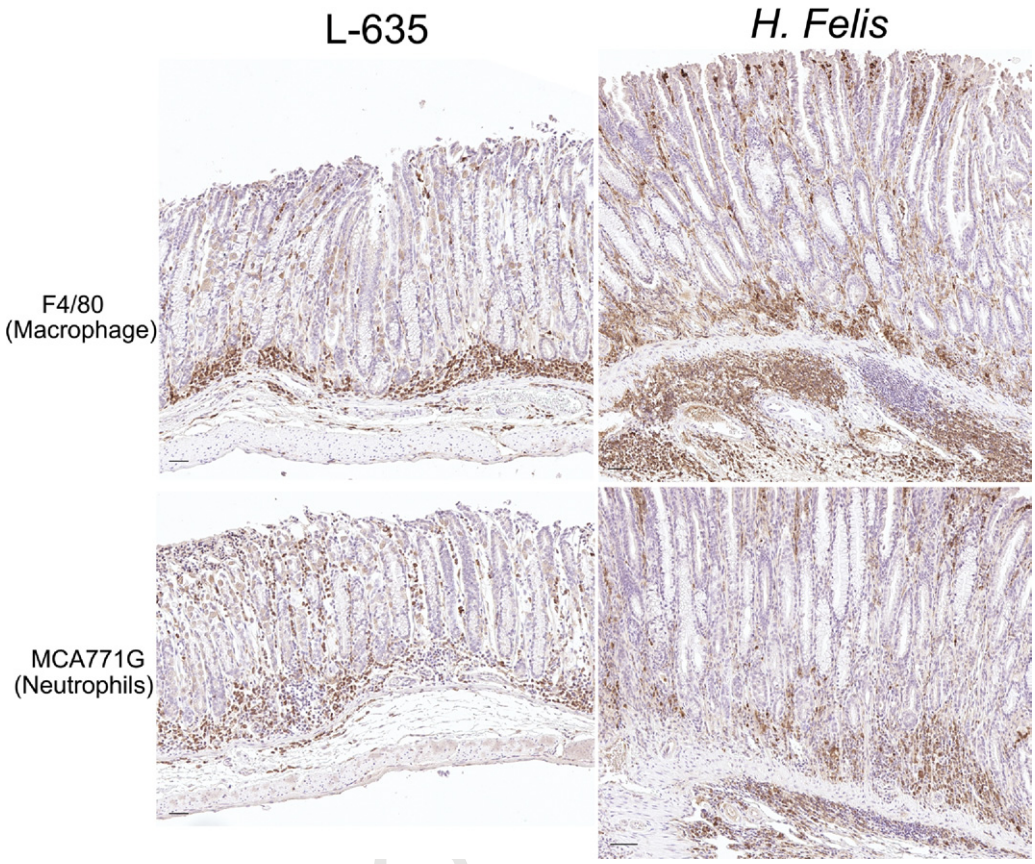

Supplementary Figure 7. Characterization of infiltrating inflammatory cells in SPEM models using macrophage and neutrophil markers. In sections of mouse stomachs from L-635–treated or *H felis*–infected mice, immunostaining was performed for F4/80, a macrophage-restricted cell surface glycoprotein antigen, and MCA771G, which recognizes a polymorphic antigen expressed by polymorphonuclear cells, but is absent on resident tissue macrophages. Both neutrophils and macrophages were observed within infiltrating inflammatory cells in both models. Bar, 50 μm.

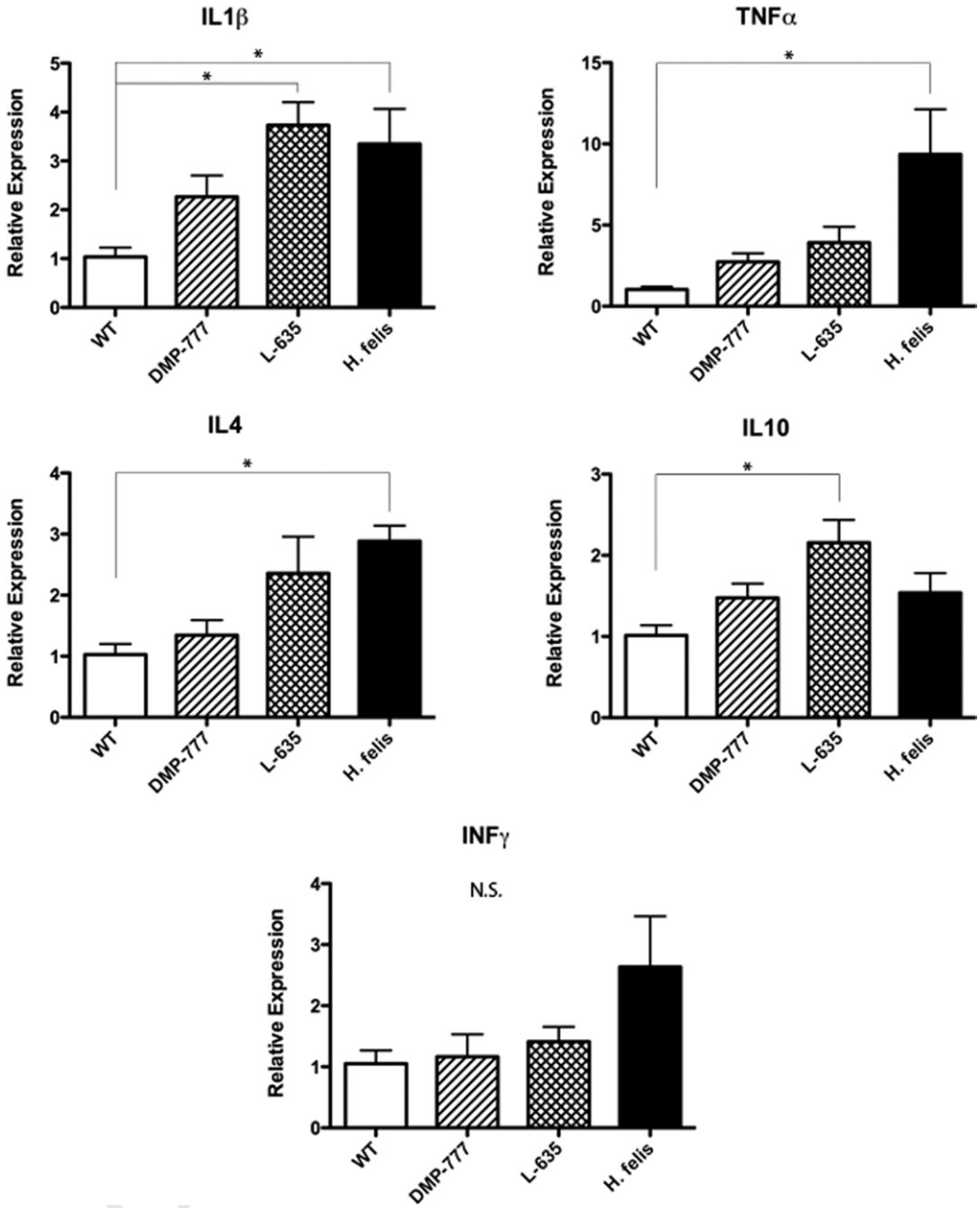

Supplementary Figure 8. Expression of cytokines in the gastric mucosa of L-635–treated and *H felis*–infected mice. Transcript levels for tumor necrosis factor (TNF)-α, IL-1β, IL-4, IL-10, and interferon-γ were determined by real-time PCR in fundic RNA samples isolated from untreated wild-type, DMP-777–treated, L-635–treated, and *H felis*–infected mice (n = 3 for all groups). Results are expressed as a ratio of the mean expression in wild-type mice (±standard error of the mean). *$P < .05$ vs untreated wild-type mice.

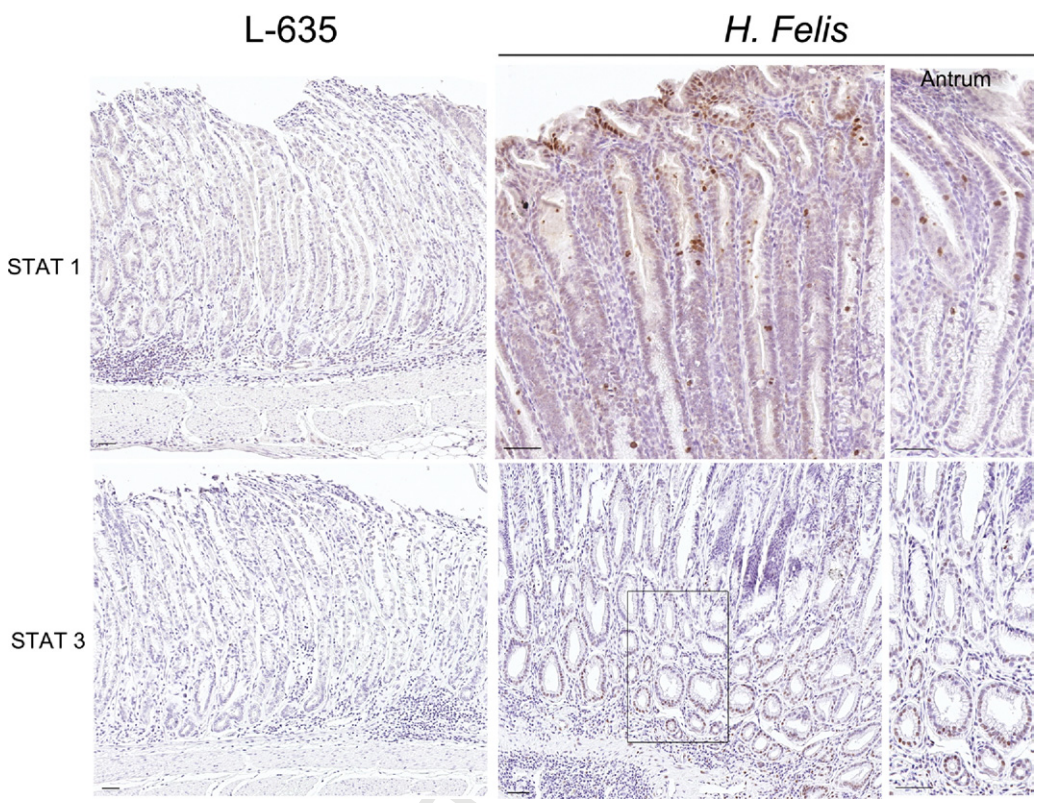

Supplementary Figure 9. The expression of cytokine receptor-associated transcription factor STATs. Sections of mouse stomachs from L-635–treated or *H felis*–infected mice were stained with antibodies against phospho-STAT1, phospho-STAT3, or phospho-STAT6. Although phospho-STAT1 and phospho-STAT3 were not activated in L-635–induced inflammatory cells, we observed activated STAT1 in both the fundus and antrum and phospho-STAT3 in the fundus in the *H felis*–infected mouse model. No phospho-STAT6 staining was observed in either model (data not shown). Bar, 50 μm.